Available online at www.sciencedirect.com
ScienceDirect
International Journal of Solids and Structures 44 (2007) 1380–1390
INTERNATIONAL JOURNAL OF SOLIDS and STRUCTURES
www.elsevier.com/locate/ijsolstr

A note on thermoelastodynamic instability (TEDI) for a 1D elastic layer: Force control

L. Afferrante *, M. Ciavarella

CEMEC-PoliBA – Centre of Excellence in Computational Mechanics, Via Re David, 200 Politecnico di Bari, 70124 Bari, Italy

Received 4 April 2006; received in revised form 14 June 2006
Available online 23 June 2006

Abstract

Recently, a new mechanism of frictional instability has been identified, for an elastic layer sliding against a rigid non-conducting support. This mechanism emerges where neither elastodynamic instabilities (e.g. 'brake squeal') nor thermoelastic ('TEI') instabilities would be active. The time scales of these processes differ considerably, so it is usual to neglect coupling between them – yet, the natural elastodynamic vibrations of the layer become unstable at arbitrarily low sliding speeds. In this paper, the force control analogous problem is treated, for which, contrary to the previous case, a pure TEI instability does not exist. The results show similar mechanisms of instability, but now the average pressure in the limit cycle is given and hence only the shape of the cycle can change.

Keywords: Thermoelastic contact; TEI; Thermoelastic instability; Squeal; Frictional vibrations

1. Introduction

Recently (Afferrante et al., 2006), a new and simple mechanism has been identified for the occurrence of frictional vibrations in which thermomechanical coupling destabilizes the lowest mode of natural vibration. The system was an elastic layer (1D model) sliding against a rigid non-conducting wall. Transient behaviour is characterized by a flutter instability at a frequency close to the first natural frequency of the elastodynamic system and it leads ultimately to a limit cycle with alternating periods of contact and separation also at this frequency. The mechanism leads to vibrations normal to the sliding interface.

This instability mechanism is distinct from that known as TEI (Barber, 1969; Dow and Burton, 1972). In this process, any perturbation in contact pressure causes a corresponding perturbation in heating and hence thermal distortion, which exaggerates the initial perturbation. Moreover, the instability mechanism is also distinct from the dynamic instabilities found by Martins et al. (1995) and Adams (1995) in the steady sliding of two elastic half-planes with elementary Coulomb friction law, which is one explanation of some of the

* Corresponding author. Tel.: +39 080 5962811; fax: +39 080 5962777.
E-mail address: luciano@poliba.it (L. Afferrante).

0020-7683/$ - see front matter
doi:10.1016/j.ijsolstr.2006.06.030

mechanisms leading to earthquakes (Ben-Zion, 2001; Rice et al., 2001), and also of 'squeal' vibrations in automotive brakes (Moirot and Nguyen, 2000).

In the present paper, we consider the elastic layer sliding in normal force control. We shall find that the same mechanism occurs, despite, in this case, TEI instability is not there and seizure is not possible.

2. Formulation

The geometry of the system is similar to that shown in Afferrante et al. (2006) (Fig. 1).

However, we now assume that a constant pressure p_0 is applied on the layer at $x = 0$. The boundary conditions hence are

$$\sigma_{xx} = -p_0; \quad \theta = 0; \quad x = 0 \tag{1}$$

$$u_x = 0; \quad K\frac{\partial\theta}{\partial x} = -fV\sigma; \quad x = h \tag{2}$$

where σ is the tensile stress and K is the thermal conductivity.

A convenient dimensionless formulation can be developed by defining the quantities

$$\xi = \frac{x}{h}; \quad \hat{t} = \frac{kt}{h^2}; \quad \widehat{V} = \frac{2\mu\alpha(1+v)fVh}{K(1-2v)}; \quad \gamma = \frac{k}{ch}$$

$$\hat{p}_0 = \frac{(1-2v)p_0}{2\mu(1-v)}; \quad \hat{u} = \frac{u_x}{h\hat{p}_0}; \quad \hat{\sigma} = \frac{\sigma}{p_0}; \quad \hat{\theta} = \frac{\alpha(1+v)\theta}{(1-v)\hat{p}_0} \tag{3}$$

where μ, v, ρ, k and α are respectively the modulus of rigidity, Poisson's ratio, density, thermal diffusivity and coefficient of expansion for the material of the layer, and

$$c = \sqrt{\frac{2\mu(1-v)}{\rho(1-2v)}} \tag{4}$$

is the dilatational wave speed. The parameter γ defines the ratio between the time scales for elastic wave propagation and for heat conduction.

In this case, Eqs. (1) and (2) reduce to

$$\hat{\sigma} = -1; \quad \hat{\theta} = 0; \quad \xi = 0 \tag{5}$$

$$\hat{u} = 0; \quad \frac{\partial\hat{\theta}}{\partial\xi} = -\widehat{V}\hat{\sigma}; \quad \xi = 1 \tag{6}$$

and

$$\frac{\partial^2\hat{\theta}}{\partial\xi^2} - \frac{\partial\hat{\theta}}{\partial\hat{t}} = 0 \tag{7}$$

$$\frac{\partial\hat{\sigma}}{\partial\xi} - \gamma^2\frac{\partial^2\hat{u}}{\partial\hat{t}^2} = 0 \tag{8}$$

$$\hat{\sigma} - \frac{\partial\hat{u}}{\partial\xi} + \hat{\theta} = 0 \tag{9}$$

are still the governing equations, in dimensionless formulation.

At the steady-state, the temperature must be a linear function of x and the stress must be constant. Therefore, we trivially obtain

$$\hat{\sigma} = -1 \tag{10}$$

$$\hat{\theta} = \widehat{V}\xi \tag{11}$$

$$\hat{u} = \frac{\widehat{V}}{2}\xi^2 - \xi + \left(1 - \frac{\widehat{V}}{2}\right) \tag{12}$$

Hence, the steady-state does not depend on the speed (contrary to the case of displacement control).

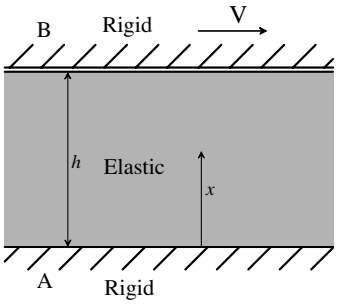

Fig. 1. An elastic layer sliding against a rigid plane surface at $x = h$ and bonded to a rigid body at $x = 0$.

2.1. Perturbation analysis

Here, we repeat the analysis done in the previous paper (Afferrante et al., 2006), where the stability of the steady-state is studied by considering the possibility that a small perturbation in the temperature and displacement fields can grow exponentially with time

$$\hat{\theta}(\xi,\hat{t}) = \hat{\theta}_0(\xi,\hat{t}) + \Theta(\xi)\exp(b\hat{t}) \tag{13}$$

$$\hat{u}(\xi,\hat{t}) = \hat{u}_0(\xi,\hat{t}) + U(\xi)\exp(b\hat{t}) \tag{14}$$

$$\hat{\sigma}(\xi,\hat{t}) = \hat{\sigma}_0(\xi,\hat{t}) + S(\xi)\exp(b\hat{t}) \tag{15}$$

where $\hat{\theta}_0$, $\hat{u}_0$ and σ_0 represent the unperturbed solution and b is the growth rate of the perturbation.

Therefore, the following characteristic equation can be derived

$$\widehat{V} = \frac{1}{\gamma}\frac{(1-\gamma^2 z^2)\cosh(z)\cosh(\gamma z^2)}{\cosh(z)\sinh(\gamma z^2) - \gamma z\sinh(z)\cosh(\gamma z^2)} \tag{16}$$

where

$$z = \sqrt{b} \tag{17}$$

If we assume that the coefficient of thermal expansion is zero, we recover the solution of the elastodynamic problem. In fact, if the coefficient of expansion $\alpha \to 0$, giving $\widehat{V} = 0$ for all finite sliding speeds, Eq. (16) reduces to

$$(1-\gamma^2 z^2)\cosh(z)\cosh(\gamma z^2) = 0 \tag{18}$$

and this has various sets of zeros. One corresponds to the factor $\cosh(z) = 0$, which gives $z = \imath(2n+1)\pi/2$ and n is an integer, corresponding to $b = -(2n+1)^2\pi^2/4$ and hence to exponentially decaying solutions of the heat conduction equation with mixed homogeneous end conditions. Also, $\cosh(\gamma z^2) = \cosh(\gamma b) = 0$ when $\gamma b = z = \imath(2n+1)\pi/2$, corresponding to oscillatory solutions which define undamped elastodynamic oscillations of the layer with fixed-free end conditions.

2.2. Zeros of the characteristic equation

The stability of the layer can be studied by finding the zeros of the characteristic equation (16) by using the method described in Afferrante et al. (2006). Alternatively, we can provide an approximate solution of the growth rate. In such case, if we redefine

$$\tilde{b} = \gamma b = \gamma z^2 \tag{19}$$

and we rewrite the characteristic equation in the following form:

$$\gamma\widehat{V}\left[\cosh\left(\sqrt{\tilde{b}/\gamma}\right)\sinh(\tilde{b}) - \gamma\sqrt{\tilde{b}/\gamma}\sinh\left(\sqrt{\tilde{b}/\gamma}\right)\cosh(\tilde{b})\right] = (1-\gamma\tilde{b})\cosh\left(\sqrt{\tilde{b}/\gamma}\right)\cosh(\tilde{b}) \tag{20}$$

When $\widehat{V} = 0$, this reduces to

$$(1 - \gamma\tilde{b})\cosh\left(\sqrt{\tilde{b}/\gamma}\right)\cosh(\tilde{b}) = 0 \tag{21}$$

where the elastodynamic modes correspond to

$$\cosh(\tilde{b}) = 0 \tag{22}$$

with solution

$$\tilde{b} = \imath(n + 1/2)\pi \tag{23}$$

Knowing the qualitative process, in which pure imaginary roots acquire a small real part, we suppose to perturb these roots slightly by writing

$$\tilde{b} = \imath(n + 1/2)\pi + \epsilon \tag{24}$$

We can then get a first approximation to the perturbed roots by perturbing the RHS of (20) to first order and replacing the LHS functions of $\tilde{b}$ by their zeroth order approximations.

After some obvious algebra, we obtain the following relation between growth rate ϵ and speed $\widehat{V}$

$$\frac{\epsilon}{\gamma\widehat{V}} = \frac{\cosh 2x + \cos 2x}{2\gamma^2\widehat{V}x(1+\imath)(\sinh x\cosh x + \imath\sin x\cos x) + (1 - \imath\gamma(n + 1/2)\pi)(\cosh 2x + \cos 2x)} \tag{25}$$

where

$$x = \sqrt{(n + 1/2)\pi/2\gamma} \tag{26}$$

For very large speed,

$$\frac{\epsilon}{\gamma} = \frac{\cosh 2x + \cos 2x}{2\gamma^2 x(1+\imath)(\sinh x\cosh x + \imath\sin x\cos x)} \tag{27}$$

which is independent on speed, whereas for very small speeds,

$$\frac{\epsilon}{\gamma\widehat{V}} = \frac{1}{(1 - \imath\gamma(n + 1/2)\pi)} \tag{28}$$

Fig. 2 shows the dependence of the exponential growth rate $\Re(b) = \Re(\epsilon)/\gamma$ on the wave number n for different dimensionless speed $\widehat{V}$ and for the first 30 modes.

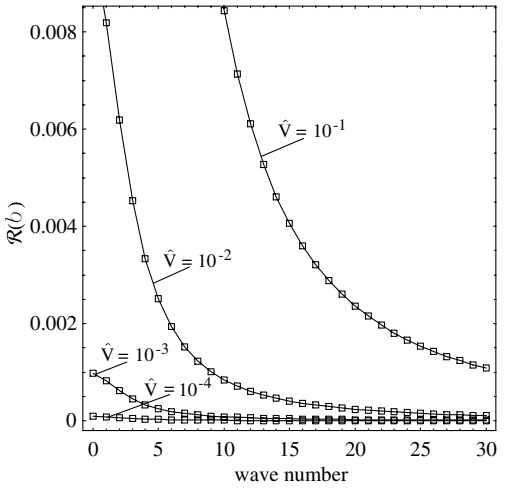

Fig. 2. Dependence of the exponential growth rate $\Re(b)$ on the wave number n, for different dimensionless speed $\widehat{V}$, the first 30 modes and $\gamma = 10^{-1}$.

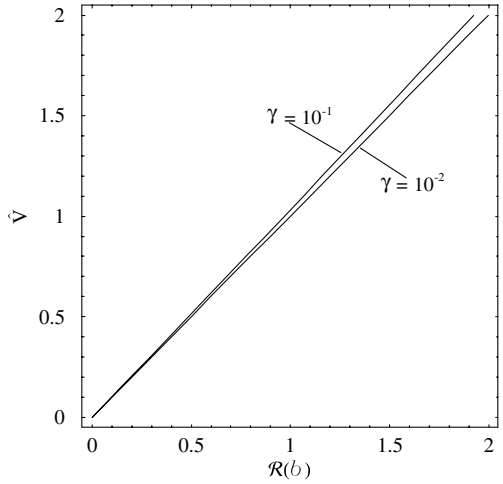

Fig. 3. Dependence of the exponential growth rate $\Re(b)$ on the dimensionless speed $\widehat{V}$, for the first mode and different γ.

The first mode is the dominant one and the growth rate very quickly reduces with n, so only the first modes characterize the stability of the layer. In Fig. 3, we plot the dependence of the exponential growth rate of the first mode on the sliding speed.

In the previous paper, we considered displacement control in the normal direction, and hence there was a well defined TEI critical speed, which was also where the quasi-static solution predicted infinite amplification of the pressure. The model with both dynamic and thermoelastic terms showed a new instability (giving rise in the long term to jumps and impacts at the interface). The instability originated at any speed and was surprisingly there also for systems having very different characteristic times of the thermal and dynamic phenomena.

Here, we control the force and find similar instabilities, but the pure TEI modes disappear (in Fig. 3, we have only complex growth factors), since in the normal direction, a quasi-static solution (like done in TEI) predicts a trivial solution which we cannot perturb in terms of pressure by definition. In the transient case, we would have again impacts and jumps, this time with "flights" of the layer above the plane. The complex roots persist for arbitrarily small γ and hardly any further change occurs in the plot of Fig. 3 for $\gamma < 10^{-2}$.

In Fig. 4, a comparison between the solution obtained with the approximate expression (28) and the 'exact' solution determined by the root finder is shown for the first mode. Notice as the approximate solution (dashed line) is very closed to the numerical one (solid line).

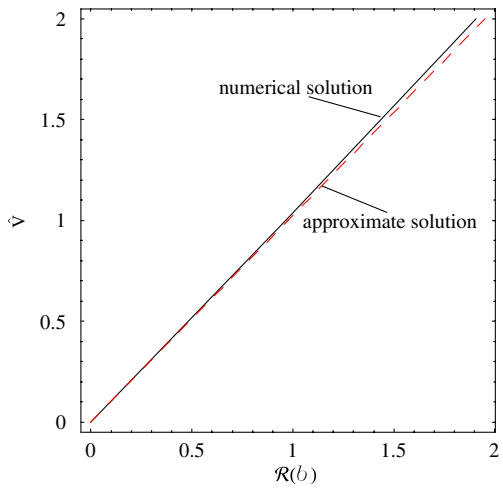

Fig. 4. Comparison between the approximate (28) and numerical solution for the first mode and $\gamma = 10^{-1}$.

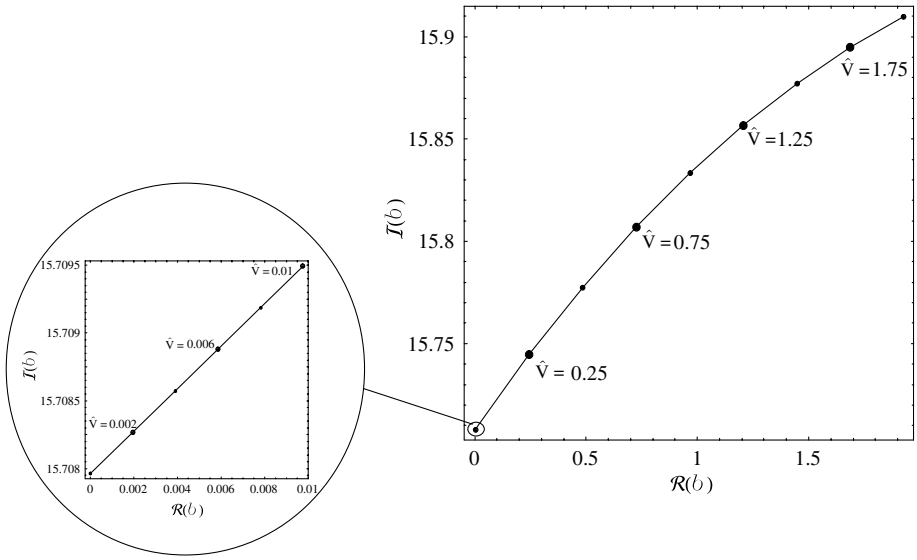

Fig. 5. Variation of the imaginary part $\Im(b)$ of the growth rate with the real part $\Re(b)$ for the first mode and $\gamma = 10^{-1}$.

Fig. 5 shows the motion of the roots in the complex plane for the first mode.

Notice that the zeros on the imaginary axis representing undamped elastodynamic oscillations of the layer, and the figures shows how they move into the unstable half-plane, as $\widehat{V}$ is increased from zero. Also, a zoom of the plot near to $\Re(b) = 0$ is given. Notice for low speeds the relation between the imaginary part $\Im(b)$ and the real part $\Re(b)$ is nearly linear.

3. Transient analysis

To explore the transient behaviour of the system, a finite difference method was employed, similarly to the case in displacement control. Details of the numerical algorithm are provided in the Appendix. The quasi-static solution predicts a monotonic transition to the steady-state (10)–(12), but the thermoelastodynamic solution predicts unstable growing oscillations. Fig. 6 shows the transient evolution of the dimensionless displacement $\hat{u}$ of the layer at $\xi = 1$ for $\gamma = 10^{-1}$ and $\widehat{V} = 0.1$.

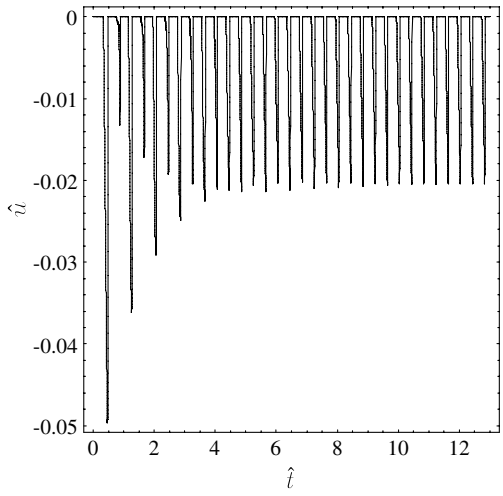

Fig. 6. Evolution of the dimensionless displacement $\hat{u}$ of the layer at $\xi = 1$ for $\gamma = 10^{-1}$ and $\widehat{V} = 0.1$.

The displacement falls to zero when the layer makes contact with the rigid wall. In particular, separation has a stabilizing effect on the process, which then tends asymptotically to a limit cycle.

In Fig. 7, the limit cycle for the contact pressure $\hat{p} = -\hat{\sigma}(1, \hat{t})$ is shown for $\gamma = 10^{-1}$ and different $\widehat{V}$. Notice as the limit cycle represents a non-linear oscillation about the quasi-static solution. However, it would seem that the main effect, even in the limit of near zero speed, is to produce a limit cycle with about 1/2 of the period in separation, and 1/2 under contact.

As secondary effect, a localized maximum appears, and the period of the steady-state oscillation slightly increases with speed, with the contact phase one reducing and the maximum pressure growing sensibly. The small reduction of pressure before the maximum value which we have at higher speed, is, probably a numerical dispersion error typical of second order discretization methods.

Fig. 8 shows the effect of the dimensionless speed $\widehat{V}$ on the maximum contact pressure $\hat{p}_{\max}$. As expected, $\hat{p}_{\max}$ monotonically increases more than linearly with $\widehat{V}$.

Finally, the forms of the pressure waves in the steady-state are sketched in Figs. 9 and 10. In particular, two waves traveling in the layer during the separation (Fig. 9) and contact (Fig. 10) period are plotted. With dashed line, we plot waves traveling from $\xi = 1$ to $\xi = 0$ and with solid line waves traveling in the opposite direction.

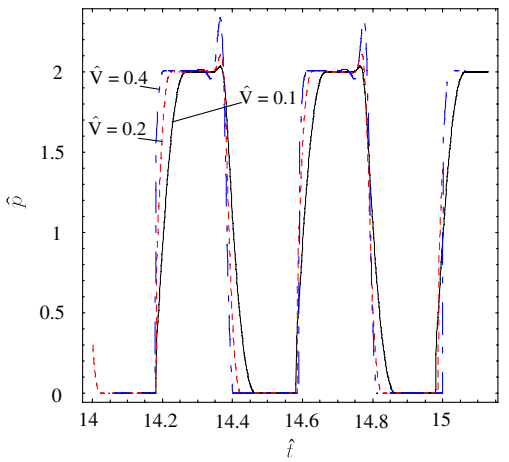

Fig. 7. Limit cycle for the contact pressure $\hat{p}$ ($\gamma = 10^{-1}$ and $\widehat{V} = 0.1, 0.2, 0.4$).

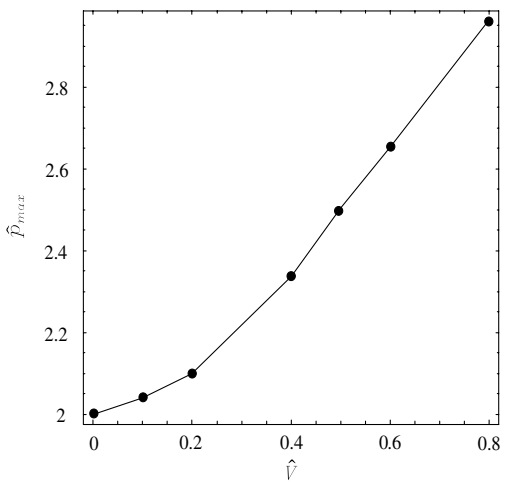

Fig. 8. Variation of $\hat{p}_{\max}$ with the speed $\widehat{V}$ for $\gamma = 10^{-1}$.

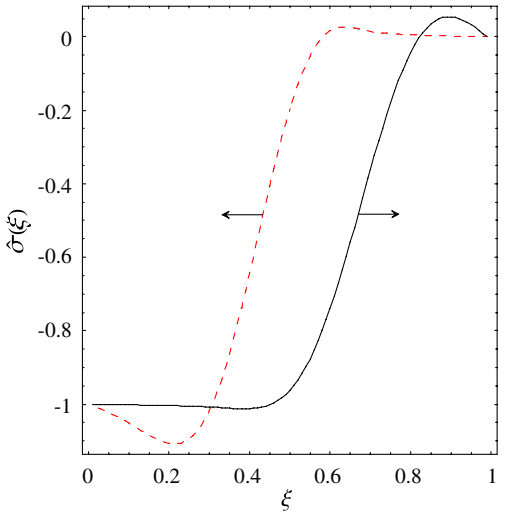

Fig. 9. Pressure waves in the steady-state during the separation phase ($\gamma = 10^{-1}$, $\widehat{V} = 0.4$).

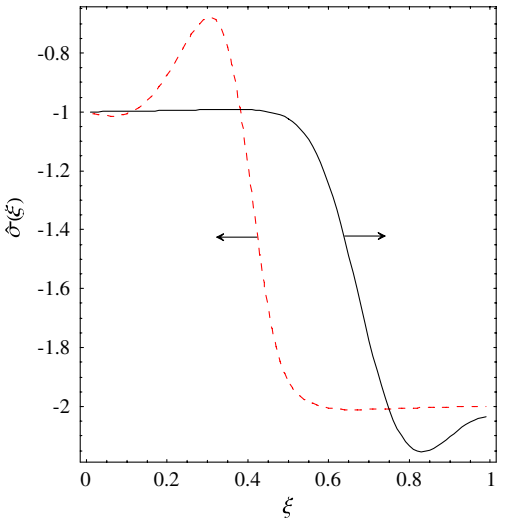

Fig. 10. Pressure waves in the steady-state during the contact phase ($\gamma = 10^{-1}$, $\widehat{V} = 0.4$).

In Fig. 9, notice that the first part of the wave traveling from $\xi = 1$ to $\xi = 0$ will reflect at $\xi = 0$ from a free end as a tensile wave. This produces the tensile region well visible in Fig. 9. Similarly, the first part of the wave traveling in the opposite direction will reflect at $\xi = 1$ as a wave of opposite sign until sufficient motion occurs to close the gap.

In Fig. 10, the wave traveling from $\xi = 0$ to $\xi = 1$ will reflect at $\xi = 1$ from a fixed end without changing your sign. The upper-pressure associated to these waves causes the peak of the pressure shown in Fig. 7.

4. Conclusions

In the study of the previous paper, under displacement control, we found a new instability which we called TEDI. This has the form of an instability of the natural dilatational modes of the layer, which in the transient regime separates and produces a non-linear limit cycle of contacts and separations. TEDI was found to be a

completely new mechanism, which makes unstable the dynamic modes, otherwise neutrally stable, due to thermoelastic effects. Dynamic instability without thermal effects would not emerge for this model, no matter how large the friction coefficient could be. However, the model in the previous paper had still a pure TEI thermoelastic instability for $\widehat{V} > \widehat{V}_{cr}$. Hence, in the present paper, to assess whether TEDI would be still present even if a pure TEI mode were not present, we wanted to clean the system even further, by considering force control, so that TEI instability is not there when thermomechanical coupling is neglected.

The analysis shows that thermomechanical coupling still destabilizes the lowest mode of natural vibration and the transient behaviour is characterized by a flutter instability. The steady-state is a limit cycle with alternating periods of contact and separation. In this case seizure is not possible, yet the maximum contact pressure continuously increases with the sliding speed $\widehat{V}$. The form of the limit cycle is different with respect to the case in displacement control. Here, the contact pressure shows a rapid rise and decay and exhibits a peak before falling to zero.

If a small amount of internal damping is introduced into the system, for example by considering a viscoelastic behaviour of the material, we expect the effect of the damping will be to reduce but not completely suppress the unstable thermoelastodynamic growth rate. In particular, a critical speed greater than zero could be introduced as a function of the damping factor.

More investigations occur for two dimensional geometries. However, here we can anticipate that the coupling between thermal and dynamic properties will destabilize the otherwise stable dynamic modes or will modify significantly those already unstable. Such considerations find a first confirmation in recent works of Yi (2006) and Afferrante and Ciavarella (2006).

Acknowledgements

The authors wish to acknowledge Prof. J.R. Barber for his helpful comments.

Appendix A. Transient formulation

We consider the following dimensionless equations to be solved (obtained by combining Eqs. (7)–(9)):

$$\frac{\partial^2\hat{\theta}}{\partial\hat{\xi}^2} - \frac{\partial\hat{\theta}}{\partial\hat{t}} = 0 \tag{29}$$

$$\frac{\partial^2\hat{u}}{\partial\hat{\xi}^2} - \gamma^2\frac{\partial^2\hat{u}}{\partial\hat{t}^2} - \frac{\partial\hat{\theta}}{\partial\hat{\xi}} = 0 \tag{30}$$

When the layer makes contact with the rigid wall B, the boundary conditions can be written in the following form:

$$\frac{\partial\hat{u}(0,\hat{t})}{\partial\hat{\xi}} - \hat{\theta}(0,\hat{t}) = 1; \quad \hat{\theta}(0,\hat{t}) = 0 \tag{31}$$

$$\hat{u}(1,\hat{t}) = 0; \quad \frac{\partial\hat{\theta}(1,\hat{t})}{\partial\hat{\xi}} = -\widehat{V}\hat{\sigma} \tag{32}$$

When separation conditions occur, we need to consider the following new boundary conditions:

$$\frac{\partial\hat{u}(0,\hat{t})}{\partial\hat{\xi}} - \hat{\theta}(0,\hat{t}) = 1; \quad \hat{\theta}(0,\hat{t}) = 0 \tag{33}$$

$$\frac{\partial\hat{u}(1,\hat{t})}{\partial\hat{\xi}} - \hat{\theta}(1,\hat{t}) = 0; \quad \frac{\partial\hat{\theta}(1,\hat{t})}{\partial\hat{\xi}} = 0 \tag{34}$$

Finally, the initial condition was taken to be quiescent with initial temperature everywhere zero i.e.

$$\hat{\theta}(\xi,0)=0 \tag{35}$$

$$\hat{u}(\xi,0)=0;\quad \frac{\partial\hat{u}(\xi,0)}{\partial\hat{t}}=0 \tag{36}$$

Wave equation

Eq. (30) is solved by using the Crank–Nicolson implicit scheme (in this way the system of finite difference equations obtained is unconditionally stable)

$$-\frac{v^2}{2}\hat{u}_{i+1}^{j+1}+(1+v^2)\hat{u}_i^{j+1}-\frac{v^2}{2}\hat{u}_{i-1}^{j+1}=\frac{v^2}{2}\hat{u}_{i+1}^{j}+2\left(1-\frac{v^2}{2}\right)\hat{u}_i^{j}+\frac{v^2}{2}\hat{u}_{i-1}^{j}-\hat{u}_i^{j-1}-v^2\left(\hat{\theta}_{i+1}^{j}-\hat{\theta}_i^{j}\right)\Delta\xi \tag{37}$$

where $v=\Delta\hat{t}/(\gamma\Delta\xi)$, $\Delta\hat{t}$ is the dimensionless time between two successive instants and $\Delta\xi$ is the dimensionless length of the elements.

In particular, the following tridiagonal system of linear algebraic equations at each new time level is obtained:

$$-\frac{v^2}{2}\hat{u}_2^{j+1}+\left(1+\frac{v^2}{2}\right)\hat{u}_1^{j+1}=C_1 \tag{38}$$

$$-\frac{v^2}{2}\hat{u}_{i+1}^{j+1}+(1+v^2)\hat{u}_i^{j+1}-\frac{v^2}{2}\hat{u}_{i-1}^{j+1}=C_i\quad i=2,\ldots,n-2 \tag{39}$$

$$(1+v^2)\hat{u}_{n-1}^{j+1}-\frac{v^2}{2}\hat{u}_{n-2}^{j+1}=C_{n-1} \tag{40}$$

where the constants C_i can be written as

$$C_1=\frac{v^2}{2}\hat{u}_2^{j}+2\left(1-\frac{v^2}{2}\right)\hat{u}_1^{j}+\frac{v^2}{2}\hat{u}_1^{j}-\hat{u}_1^{j-1}-v^2\left(\hat{\theta}_2^{j}-\hat{\theta}_1^{j}\right)\Delta\xi+v^2\Delta\xi \tag{41}$$

$$C_i=\frac{v^2}{2}\hat{u}_{i+1}^{j}+2\left(1-\frac{v^2}{2}\right)\hat{u}_i^{j}+\frac{v^2}{2}\hat{u}_{i-1}^{j}-\hat{u}_i^{j-1}-v^2\left(\hat{\theta}_{i+1}^{j}-\hat{\theta}_i^{j}\right)\Delta\xi\quad i=2,\ldots,n-2 \tag{42}$$

$$C_{n-1}=\frac{v^2}{2}\hat{u}_n^{j}+2\left(1-\frac{v^2}{2}\right)\hat{u}_{n-1}^{j}+\frac{v^2}{2}\hat{u}_{n-2}^{j}-\hat{u}_{n-1}^{j-1}-v^2\left(\hat{\theta}_n^{j}-\hat{\theta}_{n-1}^{j}\right)\Delta\xi \tag{43}$$

The above system is solved when the layer makes contact with the rigid wall B (in this case $\hat{u}(1,\hat{t})=\hat{u}_n^{j+1}=0$). When separation conditions occur the new boundary condition (34: i) involves

$$\hat{u}_n^{j+1}=\Delta\xi\hat{\theta}_n^{j+1}+\hat{u}_{n-1}^{j+1} \tag{44}$$

Consequently, we need to modify Eq. (40) in the following form:

$$\left(1+\frac{v^2}{2}\right)\hat{u}_{n-1}^{j+1}-\frac{v^2}{2}\hat{u}_{n-2}^{j+1}=\frac{v^2}{2}\hat{u}_n^{j}+2\left(1-\frac{v^2}{2}\right)\hat{u}_{n-1}^{j}+\frac{v^2}{2}\hat{u}_{n-2}^{j}-\hat{u}_{n-1}^{j-1}-v^2\left(\hat{\theta}_n^{j}-\hat{\theta}_{n-1}^{j}\right)\Delta\xi+\frac{v^2}{2}\Delta\xi\hat{\theta}_n^{j+1} \tag{45}$$

In both cases, the Thomas algorithm (Thomas, 1949) is used to solve the system of equations.

Heat equation

The heat equation (29) can be discretized in the following form (Crank–Nicolson scheme):

$$-\frac{r}{2}\hat{\theta}_{i+1}^{j+1}+(1+r)\hat{\theta}_i^{j+1}-\frac{r}{2}\hat{\theta}_{i-1}^{j+1}=\frac{r}{2}\hat{\theta}_{i+1}^{j}+(1-r)\hat{\theta}_i^{j}+\frac{r}{2}\hat{\theta}_{i-1}^{j} \tag{46}$$

where $r = \Delta\hat{t}/\Delta\xi^2$. For full sliding conditions the boundary condition at the right end of the layer can be discretized as

$$\hat{\theta}_n^{j+1} = \frac{\hat{\theta}_{n-1}^{j+1} - \widehat{V}\left(\hat{u}_n^{j+1} - \hat{u}_{n-1}^{j+1}\right)}{1 - \widehat{V}\Delta\xi} \tag{47}$$

and the equations which need to be solved are

$$-\frac{r}{2}\hat{\theta}_2^{j+1} + (1+r)\hat{\theta}_1^{j+1} = E_1 \tag{48}$$

$$-\frac{r}{2}\hat{\theta}_{i+1}^{j+1} + (1+r)\hat{\theta}_i^{j+1} - \frac{r}{2}\hat{\theta}_{i-1}^{j+1} = E_i \quad i = 2,\ldots,n-2 \tag{49}$$

$$\left(1 + r - \frac{r/2}{1 - \widehat{V}\Delta\xi}\right)\hat{\theta}_{n-1}^{j+1} - \frac{r}{2}\hat{\theta}_{n-2}^{j+1} = E_{n-1} \tag{50}$$

where

$$E_1 = \frac{r}{2}\hat{\theta}_2^{j} + (1-r)\hat{\theta}_1^{j} \tag{51}$$

$$E_i = \frac{r}{2}\hat{\theta}_{i+1}^{j} + (1-r)\hat{\theta}_i^{j} + \frac{r}{2}\hat{\theta}_{i-1}^{j} \quad i = 2,\ldots,n-2 \tag{52}$$

$$E_{n-1} = \frac{r}{2}\hat{\theta}_n^{j} + (1-r)\hat{\theta}_{n-1}^{j} + \frac{r}{2}\hat{\theta}_{n-2}^{j} - \frac{r}{2}\frac{\widehat{V}\left(\hat{u}_n^{j+1} - \hat{u}_{n-1}^{j+1}\right)}{1 - \widehat{V}\Delta\xi} \tag{53}$$

During separation periods (boundary condition at the end B of the layer involves $\hat{\theta}_n^{j+1} = \hat{\theta}_{n-1}^{j+1}$), the same equations apply, except that the terms involving $\widehat{V}$ drop and hence the modified forms of (48)–(53) can be obtained by setting $\widehat{V} = 0$.

In all the examples the layer was divided into 100 elements of equal length.

References

Adams, G.G., 1995. Self-excited oscillations of two elastic half-spaces sliding with a constant coefficient of friction. ASME J. Appl. Mech. 62, 867–872.

Afferrante, L., Ciavarella, M., 2006. Thermo-elastic Dynamic Instability (TEDI) in frictional sliding of an halfspace against a rigid non-conducting wall. J. Appl. Mech., in press.

Afferrante, L., Ciavarella, M., Barber, J.R., 2006. Sliding thermoelastodynamic instability. Proc. R. Soc. (London), A 462, 2161–2176.

Barber, J.R., 1969. Thermoelastic instabilities in the sliding of conforming solids. Proc. Roy. Soc. (London), A 312, 381–394.

Ben-Zion, Y., 2001. Dynamic ruptures in recent models of earthquake faults. J. Mech. Phys. Solids 49, 2209–2244.

Dow, T.A., Burton, R.A., 1972. Thermoelastic instability of sliding contact in the absence of wear. Wear 19, 315–328.

Martins, J.A.C., Guimaraes, J., Faria, L.O., 1995. Dynamic surface solutions in linear elasticity and viscoelasticity with frictional boundary conditions. J. Vib. Acoust. 117, 445–451.

Moirot, F., Nguyen, Q.S., 2000. Brake squeal: a problem of flutter instability of the steady sliding solution? Arch. Mech. 52, 645–662.

Rice, J.R., Lapusta, N., Ranjith, K., 2001. Rate and state dependent friction and the stability of sliding between elastically deformable solids. J. Mech. Phys. Solids 49, 1865–1898.

Thomas, L.H., 1949. Elliptic problems in linear difference equations over a network. Watson Sci. Comput. Lab. Rep., Columbia University, New York.

Yi, Y. 2006. Finite element analysis of the thermoelastodynamic instability involving frictional heating, private communication.